

A reduced basis warm-start iterative solver for the parameterized linear systems

Shijin Hou* Yanlai Chen[†] Yinhua Xia[‡]

Abstract

This paper proposes and tests the first-ever reduced basis warm-start iterative method for the parametrized linear systems, exemplified by those discretizing the parametric partial differential equations. Traditional iterative methods are usually used to obtain the high-fidelity solutions of these linear systems. However, they typically come with a significant computational cost which becomes challenging if not entirely untenable when the parametrized systems need to be solved a large number of times (e.g. corresponding to different parameter values or time steps). Classical techniques for mitigating this cost mainly include acceleration approaches such as preconditioning. This paper advocates for the generation of an initial prediction with controllable fidelity as an alternative approach to achieve the same goal. The proposed reduced basis warm-start iterative method leverages the mathematically rigorous and efficient reduced basis method to generate a high-quality initial guess thereby decreasing the number of iterative steps. Via comparison with the iterative method initialized with a zero solution and the RBM preconditioned and initialized iterative method tested on two 3D steady-state diffusion equations, we establish the efficacy of the proposed reduced basis warm-start approach.

1 Introduction

In this work, we consider the parametrized linear systems that take the general form of

$$A_h(\boldsymbol{\mu})u_h(\boldsymbol{\mu}) = f_h(\boldsymbol{\mu}), \quad (1)$$

*School of Mathematical Sciences, University of Science and Technology of China, Hefei, Anhui 230026, People's Republic of China. (houshiji@mail.ustc.edu.cn).

[†]Department of Mathematics, University of Massachusetts Dartmouth, 285 Old Westport Road, North Dartmouth, MA 02747, USA. (yanlai.chen@umassd.edu). The work of this author was partially supported by National Science Foundation grant DMS-2208277, by Air Force Office of Scientific Research grant FA9550-23-1-0037, and by the UMass Dartmouth Marine and UnderSea Technology (MUST) Research Program made possible via an Office of Naval Research grant N00014-22-1-2012.

[‡]School of Mathematical Sciences, University of Science and Technology of China, Hefei, Anhui 230026, People's Republic of China. (yhxia@ustc.edu.cn). The work of this author was partially supported by National Key R&D Program of China No. 2022YFA1005202/ 2022YFA1005200, and by National Natural Science Foundation of China grant 12271498.

where $A_h(\boldsymbol{\mu})$ denotes a parameter-dependent matrix of dimension $\mathcal{N} \times \mathcal{N}$, $u_n(\boldsymbol{\mu})$, $f_h(\boldsymbol{\mu}) \in \mathbb{R}^{\mathcal{N}}$ are \mathcal{N} -dimensional vectors, and $\boldsymbol{\mu} \in \mathcal{D} \subset \mathbb{R}^p$ is a p -dimensional parameter vector. They often stem from the discretization of parametric partial differential equations (pPDEs) whose real-time solution is widely in demand for many applications such as optimization, uncertainty quantification, and inverse problems. These systems can usually be solved with high precision by various iterative methods [20], especially when the system is large. Several classical iterative methods, such as Jacobi, Richardson, and Gauss-Seidel methods, etc, are the simplest options. They are not only used as standalone solvers but also as preconditioners for accelerating other methods. Similarly, multigrid methods (MG) have been widely developed as both iterative methods [3, 15] and preconditioners [28]. There is another class of mainstream methods, Krylov subspace methods, which includes CG [16], BiCGSTAB [29], GMRES [27], etc.

However, all these high-fidelity iterative methods depend on the full-order model (FOM) of large degrees of freedom (DoFs). Some of these systems need to be solved toward machine precision (e.g. long-time simulations in astrophysics) which means that it will take a large number of iterative steps. Both factors contribute to an extremely time-consuming process. What exacerbates the situation is that repeatedly solving such problems for different parameter instances is often necessary. It is thus imperative to design efficient and reliable solvers for such problems that converge to machine precision.

In recent decades, the reduced basis method (RBM), as a class of reduced order modeling techniques, has been developed and widely used to obtain the fast solution of pPDEs [25, 17, 14]. The RBM achieves high efficiency via an offline-online decomposition strategy and a mathematically rigorous procedure to build a surrogate solution space. In the offline phase, a reduced basis (RB) space, W_N , of dimension $N \ll \mathcal{N}$, the number of FOM DoFs, is successfully built by the greedy algorithm [26, 2] or the proper orthogonal decomposition (POD) [18, 21]. With this surrogate approximate space, a reduced-order model (ROM) can be derived that enforces the PDE at the reduced level making the ROM physics-informed as opposed to purely data-driven. Subsequently, for different values of parameters, we only need to solve the ROM with a much lower computational cost in the online phase.

In this work, we propose and test the first-ever Reduced Basis Warm-Start (RBWS) iterative method leveraging the mature RBM framework to address the cost challenge of using the traditional iterative methods to repeatedly solve parametrized linear systems. The specific RBM we employ is a highly efficient variant, the so-called L1-based reduced over-collocation (L1ROC) method [8]. After a learning stage with a bare-minimum overhead cost thanks to a cost-free L1-norm based error indicator [9], it is capable of providing a highly accurate initial prediction for the iterative methods. In essence, we are developing a data-driven warm-start approach based on the state-of-the-art physics-informed model order reduction strategies for the traditional iterative solvers for linear systems. Furthermore, we study the acceleration functionality of the RBM as a preconditioner. Via a formal analysis, we show that the approximation accuracy of the RB space of a fixed dimension, due to the need of preserving the computational efficiency, will deteriorate as the iteration goes on thus having a gradually more limited acceleration effect. In

the numerical experiments, we implement the multigrid preconditioned conjugate gradient (MGCG) method [28] and the multispace reduced basis preconditioned conjugate gradient (MSRBCG) method [11] initialized with the RB initial value. The numerical results demonstrate that the MGCG method with our proposed warm-start approach has the best performance on both convergence and efficiency.

We remark that this is by far not the first attempt to hybridize a surrogate model with a full order iterative solver. There has been a class of hybrid methods, in which the data-driven models have been employed to improve the traditional iterative methods for saving computational effort or accelerating convergence. In [30], the authors proposed a neural network warm-start approach for solving the high-frequency inverse acoustic obstacle problem. A combination of deep feedforward neural networks and convolutional autoencoders is used to establish an approximate mapping from the parameter space to the solution space that serves as a means to obtain very accurate initial predictions in [24]. In [19], the non-intrusive reduced order model was used to improve the computational efficiency of the high-fidelity nonlinear solver. In [11, 12, 23, 24], the authors proposed a multi-space reduced basis preconditioner by combining an iteration-dependent RB component that is derived from an RB solver and a fine preconditioner. Different preconditioned iterative methods such as the Richardson method and the Krylov subspace methods with this precondition have been studied. However, it's worth pointing out that these methods were not tested till machine accuracy which is the regime that a purely data-driven approach (such as the non-physics-informed neural network) or the RBM preconditioning may encounter challenges. In contrast, our proposed RBWS method does not face these challenges, and we formally analyze the limitations of the RBM preconditioning techniques.

The structure of this paper is as follows. Firstly, two iterative methods are reviewed in Section 2. In Section 3, we present the new RBWS method and analyze the limitations of the RBM preconditioning techniques. The numerical results are shown in Section 4 to demonstrate the convergence and the efficiency of the proposed method. Finally, concluding remarks are drawn in Section 5.

2 Background

This section is devoted to the review of two efficient preconditioned iterative methods for solving the linear system (1), namely, the multigrid preconditioned conjugate gradient (MGCG) method [28] and the multispace reduced basis preconditioned conjugate gradient (MSRBCG) method [11]. To start, we briefly outline the conjugate gradient method and its preconditioned version since both MGCG and MSRBCG are specific cases of the preconditioned conjugate gradient (PCG) method.

2.1 Preconditioned conjugate gradient method

The conjugate gradient (CG) method [16] was designed for solving the symmetric positive-defined linear systems. The idea is to solve the equivalent optimization problem aiming to minimize the following quadratic function

$$Q(u_h(\boldsymbol{\mu})) = \frac{1}{2}u_h^T(\boldsymbol{\mu})A_h(\boldsymbol{\mu})u_h(\boldsymbol{\mu}) - f_h^T(\boldsymbol{\mu})u_h(\boldsymbol{\mu}).$$

The CG algorithm recursively solves for the k^{th} iteration $u_h^{(k)}(\boldsymbol{\mu})$ in the k^{th} Krylov subspaces \mathcal{K}_k ,

$$u_h^{(k)}(\boldsymbol{\mu}) = \arg \min_{u_h(\boldsymbol{\mu}) \in \mathcal{K}_k} Q(u_h(\boldsymbol{\mu})).$$

The PCG method is an enhanced CG method through preconditioning. Applying a linear transformation to the original system (1) with the matrix $T(\boldsymbol{\mu})$, called the preconditioner, results in the following system

$$T^{-1}(\boldsymbol{\mu})A_h(\boldsymbol{\mu})u_h(\boldsymbol{\mu}) = T^{-1}(\boldsymbol{\mu})f_h(\boldsymbol{\mu}), \quad (2)$$

which, with an appropriately designed $T(\boldsymbol{\mu})$, features a smaller condition number than that of (1). Invoking the CG method to solve the preconditioned system (2) leads to the PCG method for (1) as presented in Algorithm 1. We denote the application of the k^{th} PCG iteration to obtain the k^{th} solution $u_h^{(k)}(\boldsymbol{\mu})$ with respect to the $(k-1)^{\text{th}}$ solution $u_h^{(k-1)}(\boldsymbol{\mu})$ by

$$u_h^{(k)}(\boldsymbol{\mu}) = \text{PCG}(A_h(\boldsymbol{\mu}), f_h(\boldsymbol{\mu}), u_h^{(k-1)}(\boldsymbol{\mu}); \mathcal{P}(\cdot)). \quad (3)$$

To describe a generic framework including the MGCG and MSRBCG algorithms presented below, we denote the preconditioner by $\mathcal{P}(\cdot)$. The vanilla version above is nothing but PCG with $\mathcal{P}(\cdot)$ defined as matrix multiplication (linear solve) with $T^{-1}(\boldsymbol{\mu})$.

2.2 Multigrid preconditioner

The multigrid (MG) method [3, 15] exploits the coarse-grid correction to overcome the limitation of the classical iterative approaches that tend to efficiently eliminate the high-frequency error, but not the low-frequency one. We consider an MG method with $J+1$ ($J \geq 1$) levels. Let $P_i(\boldsymbol{\mu})$ denotes the prolongation operator from level i to level $i+1$ with $0 \leq i \leq J$. With the finest coefficient matrix $A_h^J(\boldsymbol{\mu}) = A_h(\boldsymbol{\mu})$, then the coefficient matrix $A_h^i(\boldsymbol{\mu})$ at i^{th} level grid can be computed by $A_h^i(\boldsymbol{\mu}) = P_i^T(\boldsymbol{\mu})A_h^{i+1}(\boldsymbol{\mu})P_i(\boldsymbol{\mu})$ for $0 \leq i \leq J-1$. Considering a general equation $Au = b$, we denote

$$u_2 = S(u_1, A, b, \nu) \quad (4)$$

a smoothing step performing a smoother (Jacobi or Gauss-Seidel) ν times on u_1 to obtain u_2 . For the i^{th} -level equation $A_h^i(\boldsymbol{\mu})u_h^i(\boldsymbol{\mu}) = b(\boldsymbol{\mu})$, one iteration of the V-cycle MG method at level i is presented in Algorithm 2, denoted by $u(\boldsymbol{\mu}) = \text{MG}(b(\boldsymbol{\mu}), A_h^i(\boldsymbol{\mu}), i)$.

Algorithm 1 PCG algorithm with a generic preconditioner $\mathcal{P}(\cdot)$

- 1: **Input:** $A_h(\boldsymbol{\mu}) \in \mathbb{R}^{\mathcal{N} \times \mathcal{N}}$, $f_h(\boldsymbol{\mu}) \in \mathbb{R}^{\mathcal{N}}$, preconditioner $\mathcal{P}(\cdot)$, the residual tolerance δ , the maximum number of iterations L_{\max} and an initial value $u_h^{(0)}(\boldsymbol{\mu})$
 - 2: Compute initial residual $r_h^{(0)}(\boldsymbol{\mu}) = f_h(\boldsymbol{\mu}) - A_h(\boldsymbol{\mu})u_h^{(0)}(\boldsymbol{\mu})$ and set $k = 0$
 - 3: $s_0(\boldsymbol{\mu}) = \mathcal{P}(r_h^{(0)}(\boldsymbol{\mu}))$
 - 4: $p_0(\boldsymbol{\mu}) = s_0(\boldsymbol{\mu})$
 - 5: **while** $\|r_h^{(k)}(\boldsymbol{\mu})\|/\|f_h(\boldsymbol{\mu})\| < \delta$ & $k < L_{\max}$ **do**
 - 6: $\alpha_k(\boldsymbol{\mu}) = \frac{(r_h^{(k)}(\boldsymbol{\mu}))^T s_k(\boldsymbol{\mu})}{p_k^T(\boldsymbol{\mu})A_h(\boldsymbol{\mu})p_k(\boldsymbol{\mu})}$
 - 7: $u_h^{(k+1)}(\boldsymbol{\mu}) = u_h^{(k)}(\boldsymbol{\mu}) + \alpha_k(\boldsymbol{\mu})p_k(\boldsymbol{\mu})$
 - 8: $r_h^{(k+1)}(\boldsymbol{\mu}) = r_h^{(k)}(\boldsymbol{\mu}) - \alpha_k(\boldsymbol{\mu})A_h(\boldsymbol{\mu})p_k(\boldsymbol{\mu})$
 - 9: $s_{k+1}(\boldsymbol{\mu}) = \mathcal{P}(r_h^{(k+1)}(\boldsymbol{\mu}))$
 - 10: $\beta_k(\boldsymbol{\mu}) = \frac{(r_h^{(k+1)}(\boldsymbol{\mu}))^T s_{k+1}(\boldsymbol{\mu})}{(r_h^{(k)}(\boldsymbol{\mu}))^T s_k(\boldsymbol{\mu})}$
 - 11: $p_{k+1}(\boldsymbol{\mu}) = s_{k+1}(\boldsymbol{\mu}) + \beta_k(\boldsymbol{\mu})p_k(\boldsymbol{\mu})$
 - 12: $k = k + 1$
 - 13: **end while**
-

Using the MG method as a preconditioner of the PCG method, i.e., replacing the Step 9 of Algorithm 1 by $s_{k+1}(\boldsymbol{\mu}) = \text{MG}(r_h^{(k+1)}(\boldsymbol{\mu}), A_h(\boldsymbol{\mu}), J)$, we obtain the MGCG method.

$$\text{MGCG}(A_h(\boldsymbol{\mu}), f_h(\boldsymbol{\mu}), u_h^{(k-1)}(\boldsymbol{\mu})) := \text{PCG}(A_h(\boldsymbol{\mu}), f_h(\boldsymbol{\mu}), u_h^{(k-1)}(\boldsymbol{\mu}); \text{MG}(\cdot, A_h(\boldsymbol{\mu}), J)).$$

Algorithm 2 MG V-cycle at level i : $u(\boldsymbol{\mu}) = \text{MG}(b(\boldsymbol{\mu}), A_h^i(\boldsymbol{\mu}), i)$

- 1: **Input:** $\{A_h^i(\boldsymbol{\mu})\}_{i=0}^J$, $\{p_i(\boldsymbol{\mu})\}_{i=0}^{J-1}$, $b(\boldsymbol{\mu})$, the number of pre-smoothing steps ν , and level i
 - 2: Implement the pre-smoothing process $\tilde{u}(\boldsymbol{\mu}) = S(0, A_h^i(\boldsymbol{\mu}), b(\boldsymbol{\mu}), \nu)$
 - 3: Compute residual $r_i(\boldsymbol{\mu}) = b(\boldsymbol{\mu}) - A_h^i(\boldsymbol{\mu})\tilde{u}(\boldsymbol{\mu})$
 - 4: Restrict residual $r_{i-1}(\boldsymbol{\mu}) = p_{i-1}^T(\boldsymbol{\mu})r_i(\boldsymbol{\mu})$
 - 5: Correct the error on the coarse grid:
 if $i = 1$, $e_0(\boldsymbol{\mu}) = (A_h^0(\boldsymbol{\mu}))^{-1}r_0(\boldsymbol{\mu})$
 else $e_{i-1}(\boldsymbol{\mu}) = \text{MG}(r_{i-1}(\boldsymbol{\mu}), A_h^{i-1}(\boldsymbol{\mu}), i - 1)$
 - 6: Prolongate coarse grid correction $\bar{u}(\boldsymbol{\mu}) = \tilde{u}(\boldsymbol{\mu}) + p_{i-1}(\boldsymbol{\mu})e_{i-1}(\boldsymbol{\mu})$
 - 7: Implement the post-smoothing process $u(\boldsymbol{\mu}) = S(\bar{u}(\boldsymbol{\mu}), A_h^i(\boldsymbol{\mu}), b(\boldsymbol{\mu}), \nu)$
-

2.3 Multispace reduced basis preconditioner

Multispace reduced basis (MSRB) preconditioner [11] combines a fine grid preconditioner, such as Jacobi and Gauss-Seidel preconditioner with a coarse preconditioner induced from a reduced basis solver. We consider the equation $A_h(\boldsymbol{\mu})u_h(\boldsymbol{\mu}) = b(\boldsymbol{\mu})$.

With n_s snapshots $\{u_h(\boldsymbol{\mu}_i)\}_{i=1}^{n_s}$ (that are the high-fidelity solutions computed for the training parameters $\Xi_{\text{train}} = \{\boldsymbol{\mu}_i\}_{i=1}^{n_s}$), the proper orthogonal decomposition (POD) is used to build the RB space of dimension N , represented by the column space of a matrix $W_N = [w_1, \dots, w_N] \in \mathbb{R}^{\mathcal{N} \times N}$. Then we can obtain an RB approximation $u_h^{rb}(\boldsymbol{\mu}) = W_N u_N(\boldsymbol{\mu})$ by solving the following reduced linear system

$$A_N(\boldsymbol{\mu})u_N(\boldsymbol{\mu}) = b_N(\boldsymbol{\mu}). \quad (5)$$

where $A_N(\boldsymbol{\mu}) \in \mathbb{R}^{N \times N}$ and $b_N(\boldsymbol{\mu}) \in \mathbb{R}^N$ are obtained by projecting $A_h(\boldsymbol{\mu})$ and $b(\boldsymbol{\mu})$ to the RB space

$$A_N(\boldsymbol{\mu}) = W_N^T A_h(\boldsymbol{\mu}) W_N, \quad b_N(\boldsymbol{\mu}) = W_N^T b(\boldsymbol{\mu}).$$

Thus the RB solution can be expressed as

$$u_h^{rb}(\boldsymbol{\mu}) = W_N A_N^{-1}(\boldsymbol{\mu}) b_N(\boldsymbol{\mu}).$$

Let the application of the above POD-based RBM with the RB dimension N be denoted by

$$u_h^{rb}(\boldsymbol{\mu}) = \text{RBM}_{\text{POD}}(A_h(\boldsymbol{\mu}), b(\boldsymbol{\mu}), N). \quad (6)$$

Combining a fine smoother denoted as (4) with the RB preconditioner (6), the MSRB preconditioner is presented in Algorithm 3, denoted by $u(\boldsymbol{\mu}) = \text{MSRB}(b(\boldsymbol{\mu}), A_h(\boldsymbol{\mu}), N)$. Replacing the Step 9 of Algorithm 1 by $s_{k+1}(\boldsymbol{\mu}) = \text{MSRB}(r_h^{(k+1)}(\boldsymbol{\mu}), A_h(\boldsymbol{\mu}), N^{(k)})$ gives the MSRBCG method:

$$\text{MSRBCG}(A_h(\boldsymbol{\mu}), f_h(\boldsymbol{\mu}), u_h^{(k-1)}(\boldsymbol{\mu})) := \text{PCG}(A_h(\boldsymbol{\mu}), f_h(\boldsymbol{\mu}), u_h^{(k-1)}(\boldsymbol{\mu}); \text{MSRB}(\cdot, A_h(\boldsymbol{\mu}), N^{(k)})).$$

Here the k^{th} RB space $W_{N^{(k)}}$ of dimension $N^{(k)}$ needs to be specifically built based on the error snapshots $\{e_h^{(k)}(\boldsymbol{\mu}_i)\}_{i=1}^{n_s}$ that are the high-fidelity solutions of the k^{th} error equation $A_h(\boldsymbol{\mu})e_h^{(k)}(\boldsymbol{\mu}) = r_h^{(k)}(\boldsymbol{\mu})$.

Algorithm 3 MSRB preconditioner with W_N : $u(\boldsymbol{\mu}) = \text{MSRB}(b(\boldsymbol{\mu}), A_h(\boldsymbol{\mu}), N)$

- 1: **Input:** $A_h(\boldsymbol{\mu}) \in \mathbb{R}^{\mathcal{N} \times \mathcal{N}}$, $b(\boldsymbol{\mu}) \in \mathbb{R}^{\mathcal{N}}$, and the RB dimension N
 - 2: Implement the fine-smoothing process $\tilde{u}(\boldsymbol{\mu}) = S(0, A_h(\boldsymbol{\mu}), b(\boldsymbol{\mu}), 1)$
 - 3: Compute residual $r(\boldsymbol{\mu}) = b(\boldsymbol{\mu}) - A_h(\boldsymbol{\mu})\tilde{u}(\boldsymbol{\mu})$
 - 4: compute $u_h^{rb}(\boldsymbol{\mu}) = \text{RBM}_{\text{POD}}(A_h(\boldsymbol{\mu}), r(\boldsymbol{\mu}), N)$
 - 5: Update $u(\boldsymbol{\mu}) = \tilde{u}(\boldsymbol{\mu}) + u_h^{rb}(\boldsymbol{\mu})$
-

3 Reduced basis warm-start iterative solvers

In this section, we present the reduced basis warm-start iterative method. The method relies on the L1-based reduced over-collocation (L1ROC) method [7, 8], a highly efficient variant of the reduced basis method, to provide a controllable high-quality initial

prediction. The PCG method presented in Algorithm 1 is then used for refining the RB initialization. To provide some theoretical and intuitive footing of the new method's superior performance over the MSRBCG algorithm, we provide a formal analysis of the MSRB preconditioner presented in Algorithm 3.

3.1 L1-based reduced over-collocation method

The L1ROC method is a greedy-based reduced basis method, where a greedy algorithm adaptively chooses snapshots by finding the parameter location at which the error estimate is maximum. This sequential sampling framework and its avoidance of truncation after POD-type pervasive sampling make the algorithm highly efficient and much less data-intensive.

Two key points further ensure the high efficiency of the L1ROC method. First is the direct adoption as the online solver of the discrete empirical interpolation method (DEIM) [5, 1]. Assume we have built a RB matrix $W_N = [w_1, \dots, w_N] \in \mathbb{R}^{N \times N}$, and a set of collocation points $X^M = \{x_1, \dots, x_M\}$ ($M = 2N - 1$). We denote by $\chi = [\chi_1, \dots, \chi_M]$ the subset of the entries corresponding to the points X^M . For simplicity of notation, we introduce a sub-sampling matrix as

$$P = [\mathbf{e}_{\chi_1}, \dots, \mathbf{e}_{\chi_M}]^T \in \mathbb{R}^{M \times N},$$

where $\mathbf{e}_{\chi_i} = [0, \dots, 0, 1, 0, \dots, 0]^T \in \mathbb{R}^N$ denotes the unit vector whose χ_i -th component equals 1. Then the RB approximation $u_h^{rb}(\boldsymbol{\mu}) = W_N u_N(\boldsymbol{\mu})$ is given by solving the minimum square error estimate of the following sub-sampled system

$$P A_h(\boldsymbol{\mu}) W_N u_N(\boldsymbol{\mu}) \approx P b(\boldsymbol{\mu}), \quad (7)$$

namely,

$$u_N(\boldsymbol{\mu}) = \arg \max_{c \in \mathbb{R}^N} \|P(b(\boldsymbol{\mu}) - A_h(\boldsymbol{\mu}) W_N c)\|_{\mathbb{R}^M}.$$

The other point is the proposal of an efficient error indicator that relies on the L1 norm of the RB coefficient with respect to the chosen snapshots [9]. Assume we have selected n parameters $\{\boldsymbol{\mu}_{l_i}\}_{i=1}^n$ from the training parameter set $\Xi_{\text{train}} = \{\boldsymbol{\mu}_i\}_{i=1}^{n_s}$ and obtained the snapshots $\{u_h(\boldsymbol{\mu}_{l_i})\}_{i=1}^n$ (that are unorthogonalized RB vectors). With the RB matrix $U_n = [u_h(\boldsymbol{\mu}_{l_1}), \dots, u_h(\boldsymbol{\mu}_{l_n})]$, the RB approximation $u_h^{rb}(\boldsymbol{\mu})$ can be represented as $u_h^{rb}(\boldsymbol{\mu}) = U_n c_n(\boldsymbol{\mu})$. The L1-based error indicator is presented as follows

$$\Delta_n^{L1}(\boldsymbol{\mu}) = \|c_n(\boldsymbol{\mu})\|_{l_1}.$$

Based on this, the RB space W_N and the collocation points X^M are built by a greedy algorithm efficiently, which is presented in Algorithm 4. Note that

$$(u_n, x_*^n) = \text{DEIM}(W_{n-1}, u_h(\boldsymbol{\mu}_{l_n}))$$

in Step 7 denotes the application of the DEIM process on a new snapshot $u_h(\boldsymbol{\mu}_{l_n})$ with respect to the previous RB space W_{n-1} . The return result u_n is the orthonormal (under

point evaluation) RB vector and x_\star^n is the corresponding interpolation point. We denote the application of the L1ROC method including the offline and online process by

$$u_h^{rb}(\boldsymbol{\mu}) = \text{RBM}_{\text{L1ROC}}(A_h(\boldsymbol{\mu}), b(\boldsymbol{\mu}), N). \quad (8)$$

Algorithm 4 Offline algorithm for L1ROC

- 1: **Input:** The training parameter set Ξ_{train} and the dimension of the RB space N
 - 2: Initialize $W_0 = R_0 = X_s^0 = X_r^0 = \emptyset$
 - 3: Choose $\boldsymbol{\mu}_{l_1}$ randomly in Ξ_{train} and obtain $u_h(\boldsymbol{\mu}_{l_1})$ by Algorithm 1. Find $(u_1, x_\star^1) = \text{DEIM}(W_0, u_h(\boldsymbol{\mu}_{l_1}))$. Then let $n = 1$, $m = 1$, $X_s^n = \{x_\star^1\}$, $X_r^m = X_s^n \cup X_r^{n-1}$ and $W_1 = [u_1]$.
 - 4: **for** $n = 2, \dots, N$ **do**
 - 5: Solve $u_{n-1}(\boldsymbol{\mu})$ by the system (7) with W_{n-1}, X^m and calculate Δ_{n-1}^{L1} for every $\boldsymbol{\mu} \in \Xi_{\text{train}}$.
 - 6: Find $\boldsymbol{\mu}_{l_n} = \arg \max_{\boldsymbol{\mu} \in \Xi_{\text{train}}} \Delta_{n-1}^{L1}(\boldsymbol{\mu})$.
 - 7: Solve $u_h(\boldsymbol{\mu}_{l_n})$ by Algorithm 1. Find $(u_n, x_\star^n) = \text{DEIM}(W_{n-1}, u_h(\boldsymbol{\mu}_{l_n}))$ and let $X_s^n = X_s^{n-1} \cup \{x_\star^n\}$.
 - 8: Compute $r_{n-1}(\boldsymbol{\mu}_{l_n}) = b(\boldsymbol{\mu}_{l_n}) - A_h(\boldsymbol{\mu}_{l_n})W_{n-1}u_{n-1}(\boldsymbol{\mu}_{l_n})$. Find $(r_{n-1}, x_{\star\star}^{n-1}) = \text{DEIM}(R_{n-2}, r_{n-1}(\boldsymbol{\mu}_{l_n}))$ and let $X_r^{n-1} = X_r^{n-2} \cup \{x_{\star\star}^{n-1}\}$.
 - 9: Update $W_n = [W_{n-1}, u_n]$, $m = m + 2$, $X^m = X_s^n \cup X_r^{n-1}$.
 - 10: **end for**
-

3.2 Main algorithm

Inspired by the neural network warm-start approaches [30, 24] and afforded by the highly efficient online solver of the L1ROC method, we introduce the Reduced Basis Warm-Start (RBWS) iterative method. It features an offline training process which adds minimum overhead cost thanks to the adoption of the highly efficient L1ROC method. After this training stage, RBWS employs the L1ROC online solver to generate an accurate RB solution for each new system as the initial value. Then the PCG method presented in Algorithm 1 is applied to refine the initial value towards the exact solution.

This RBM initialized PCG (RBI-PCG) method is presented in Algorithm 5, where either (6) or (8) can be adopted as $\text{RBM}(A_h(\boldsymbol{\mu}), f_h(\boldsymbol{\mu}), N)$. Depending on what specific $\mathcal{P}(\cdot)$ the algorithm takes, it leads to the RBM initialized MGCG (RBI-MGCG) method or the RBM initialized MSRBCG (RBI-MSRBCG) method when replacing the $\mathcal{P}(\cdot)$ in Step 5 by the MG method of Algorithm 2 or the MSRB of Algorithm 3.

3.2.1 MSRB Update: Factors toward its low efficiency.

In this section, we aim to provide some insight into the performance of the MSRB preconditioner described in Section 2.3 in the RBM-initialized iterative method for the

Algorithm 5 RBI-PCG algorithm, generating RBI-MGCG and RBI-MSRBCG

- 1: **Input:** $A_h(\boldsymbol{\mu}) \in \mathbb{R}^{N \times N}$, $f_h(\boldsymbol{\mu}) \in \mathbb{R}^N$, the RB dimension N , the residual tolerance δ , and the maximum number of iterations L_{\max}
 - 2: Generate an initial value by solving the RB system: $u_h^{(0)}(\boldsymbol{\mu}) = \text{RBM}(A_h(\boldsymbol{\mu}), f_h(\boldsymbol{\mu}), N)$
 - 3: Compute initial residual $r_h^{(0)}(\boldsymbol{\mu}) = f_h(\boldsymbol{\mu}) - A_h(\boldsymbol{\mu})u_h^{(0)}(\boldsymbol{\mu})$ and set $k = 0$
 - 4: **while** $\|r_h^{(k)}(\boldsymbol{\mu})\|/\|f_h(\boldsymbol{\mu})\| < \delta$ & $k < L_{\max}$ **do**
 - 5: $u_h^{(k)}(\boldsymbol{\mu}) = \text{PCG}(A_h(\boldsymbol{\mu}), f_h(\boldsymbol{\mu}), u_h^{(k-1)}(\boldsymbol{\mu}); \mathcal{P}(\cdot))$
 - 6: $r_h^{(k)}(\boldsymbol{\mu}) = f_h(\boldsymbol{\mu}) - A_h(\boldsymbol{\mu})u_h^{(k)}(\boldsymbol{\mu})$
 - 7: $k = k + 1$
 - 8: **end while**
-

high-precision solution. For simplicity, we consider the MSRB preconditioned Richardson method that is easily rewritten as

$$\begin{cases} u_h^{(0)}(\boldsymbol{\mu}) = \text{RBM}(A_h(\boldsymbol{\mu}), f_h(\boldsymbol{\mu}), N), \\ u_h^{(k-\frac{1}{2})}(\boldsymbol{\mu}) = u_h^{(k-1)}(\boldsymbol{\mu}) + S(0, A_h(\boldsymbol{\mu}), r_h^{(k-1)}(\boldsymbol{\mu}), 1), \quad k = 1, 2, \dots, \\ u_h^{(k)}(\boldsymbol{\mu}) = u_h^{(k-\frac{1}{2})}(\boldsymbol{\mu}) + \text{RBM}(A_h(\boldsymbol{\mu}), r_h^{(k-\frac{1}{2})}(\boldsymbol{\mu}), N^{(k)}), \quad k = 1, 2, \dots \end{cases} \quad (9)$$

Here $r_h^{(l)}(\boldsymbol{\mu}) = f_h(\boldsymbol{\mu}) - A_h(\boldsymbol{\mu})u_h^{(l)}(\boldsymbol{\mu})$ denotes the residual corresponding to the iterative solution $u_h^{(l)}(\boldsymbol{\mu})$. The method relies on corrections afforded by the resolution of the error equations where we denote the error of the k^{th} iterative solution by $e_h^{(k)}(\boldsymbol{\mu}) = u_h(\boldsymbol{\mu}) - u_h^{(k)}(\boldsymbol{\mu})$

$$\begin{cases} A_h(\boldsymbol{\mu})e_h^{(k-1)}(\boldsymbol{\mu}) = r_h^{(k-1)}(\boldsymbol{\mu}) & \text{(by the smoother)} \\ A_h(\boldsymbol{\mu})e_h^{(k-\frac{1}{2})}(\boldsymbol{\mu}) = r_h^{(k-\frac{1}{2})}(\boldsymbol{\mu}) & \text{(by the RBM online solver).} \end{cases} \quad (10)$$

The first one is a full order model that is, albeit expensive, well-known (e.g. Multi-grid literature) to be effective in driving the approximation to convergence. However, the second one, less well-understood, relies on *the low-rank approximability of the error manifold*. This strategy comes with two challenges.

1. Improving accuracy requirement on RBM as $k \uparrow$. Because this is a correction step for $u_h^{(k-\frac{1}{2})}(\boldsymbol{\mu})$, its accuracy should be above the error committed by $u_h^{(k-\frac{1}{2})}(\boldsymbol{\mu})$. As shown by the next lemma, this means that the RB dimension will have to increase with respect to the iteration index k .

Lemma 3.1. *Given that the linear system is well-conditioned and the Kolmogorov n -width of the error manifold*

$$\mathcal{W} := \{A_h(\boldsymbol{\mu})^{-1}(r_h^{(k-\frac{1}{2})}(\boldsymbol{\mu})) : \boldsymbol{\mu} \in \mathcal{D}\}$$

decreases at a polynomial or exponential rate uniformly with respect to k , it follows that the dimension n of the reduced basis manifold must increase as the iteration index k increases.

Proof. It is easy to see, from (9), that

$$e_h^{(k)}(\boldsymbol{\mu}) = e_h^{(k-\frac{1}{2})}(\boldsymbol{\mu}) - \tilde{e}_h^{(k-\frac{1}{2})}(\boldsymbol{\mu})$$

where $\tilde{e}_h^{(k-\frac{1}{2})}(\boldsymbol{\mu})$ represents the (n -dimensional) RBM online approximation of $e_h^{(k-\frac{1}{2})}(\boldsymbol{\mu})$ by (10). This is lower-bounded by the best approximation error

$$\|e_h^{(k-\frac{1}{2})}(\boldsymbol{\mu}) - P_{W_n} e_h^{(k-\frac{1}{2})}(\boldsymbol{\mu})\| \leq \sigma_n(\mathcal{W}) := \max_{w \in \mathcal{W}} \|w - P_{W_n} w\|$$

where P_{W_n} denotes the projection into the RB space W_n . We have that, with the RBM greedy algorithm, $\sigma_n(\mathcal{W})$ inherits the same rate of decay of the Kolmogorov n -width $d_n(\mathcal{W})$ as follows[2]¹ :

- **Polynomial decay.** If $d_n(\mathcal{W}) \approx Mn^{-\alpha}$, then $\sigma_n(\mathcal{W}) \approx CMn^{-\alpha}$ with $C := q^{\frac{1}{2}}(4q)^\alpha$ and $q := \lceil 2^{\alpha+1}\gamma^{-1} \rceil^2$. Here $M := \max_{w \in \mathcal{W}} \|w\|$ and γ is the norm-equivalency constant between $\|\cdot\|$ and the error estimator adopted by the RBM. Given that $A_h(\boldsymbol{\mu})$ is well-conditioned, we have $M = \gamma^{-1} \left(\max_{\boldsymbol{\mu} \in \mathcal{D}} \|r_h^{(k-\frac{1}{2})}(\boldsymbol{\mu})\| \right)$ and therefore

$$\|e_h^{(k)}(\boldsymbol{\mu})\| \approx C\gamma^{-1} \left(\max_{\boldsymbol{\mu} \in \mathcal{D}} \|r_h^{(k-\frac{1}{2})}(\boldsymbol{\mu})\| \right) n^{-\alpha}.$$

Given that C is dependent on α (which is assumed to be uniform with k) and γ (which is determined solely by $A_h(\boldsymbol{\mu})$), we conclude that for $\|e_h^{(k)}(\boldsymbol{\mu})\|$ to decay with respect to k , the RB dimension n should increase as k increases (i.e. the iteration goes on).

- **Exponential decay.** The result follows similarly as in the case of polynomial decay thanks to the inheritance of the decay rate of $\sigma_n(\mathcal{W})$ proved in [2].

□

2. Degradation of the low-rank structure. We first define the residual manifold at step k

$$\mathcal{R}^{(k)} := \left\{ r_h^{(k-\frac{1}{2})}(\boldsymbol{\mu}) = f_h(\boldsymbol{\mu}) - A_h(\boldsymbol{\mu})u_h^{(k-\frac{1}{2})}(\boldsymbol{\mu}) : \boldsymbol{\mu} \in \mathcal{D} \right\}.$$

As k increases and $u_h^{(k-\frac{1}{2})}(\boldsymbol{\mu})$ gets more accurate, $\|r_h^{(k-\frac{1}{2})}(\boldsymbol{\mu})\|$ decreases. Since we aim to have $\|r_h^{(k-\frac{1}{2})}(\boldsymbol{\mu})\|$ at the level of machine accuracy at convergence, elements of $r_h^{(k-\frac{1}{2})}(\boldsymbol{\mu})$

¹To simplify our formal analysis, we assume that the upper bounds on the decay rates in [2] are actually attainable, as typically confirmed numerically in the RBM literature.

will become more and more comparable to the round off error. This means that the Kolmogorov n -width

$$d_n^k := d_n(\mathcal{R}^{(k)})$$

will likely decay slower as k increases. While this is confirmed by our numerical results (see Figure 3 which also shows the decay rates for the residual manifolds), we intend to leave the theoretical proof of this degradation to future work.

Remark 3.1. *The compounding impact of the two challenges enunciated above is that the RB space dimension must increase significantly as the iteration proceeds if we were to maintain the convergence rate of the iterative solver. However, this comes with a significant cost (see Appendix A) making the preconditioning not cost-effective. On the other hand, if we aim to control the computational cost (by e.g. fixing the RB dimension), the convergence rate will deteriorate as the iterative solver proceeds. This is confirmed by our numerical results next - the convergence of the RBWS does not deteriorate while the RBI-MSRBCG does.*

4 Numerical tests

To test our algorithms, we set $\Omega = (0, 1)^3$ with non-intersecting boundaries Γ_D and Γ_N such that $\partial\Omega = \Gamma_D \cup \Gamma_N$. We consider the following parametrized diffusion equation

$$\begin{cases} -\nabla \cdot (\mathcal{K}(\boldsymbol{\mu}) \nabla u(\boldsymbol{\mu})) = f(\boldsymbol{\mu}), & \text{in } \Omega, \\ u(\boldsymbol{\mu}) = g_D(\boldsymbol{\mu}), & \text{on } \Gamma_D, \\ \frac{\partial u(\boldsymbol{\mu})}{\partial n} = g_N(\boldsymbol{\mu}), & \text{on } \Gamma_N. \end{cases} \quad (11)$$

Here, the diffusion tensor $\mathcal{K}(\boldsymbol{\mu})$, the source term $f(\boldsymbol{\mu})$, and the boundary conditions $g_D(\boldsymbol{\mu})$, $g_N(\boldsymbol{\mu})$ may depend on parameter $\boldsymbol{\mu} \in \mathcal{D}$. Specifically, the following two examples are given as considered in [23, 11] respectively.

Example 1 Dirichlet boundary value problem where the specific definitions are given by

$$\mathcal{K}(\boldsymbol{\mu}) = 1 + \mu_1 (\sin(20\pi(4(x - \frac{1}{2})^2 + (y - \frac{1}{2})^2 + (z - \frac{1}{2})^2)))^2,$$

$$f = 3\pi^2 \sin(\pi x) \sin(\pi y) \sin(\pi z)$$

$$g_D(\boldsymbol{\mu}) = (1 - \mu_2) \cos(10\pi(4(x - \frac{1}{2})^2 + (y - \frac{1}{2})^2 + (z - \frac{1}{2})^2)) + \mu_2 \cos(10\pi(x + y + z)).$$

The parameter domain is $\mathcal{D} = [0, 2] \times [0, 1]$.

Example 2 Mixed boundary value problem

$$\Gamma_N = \{\mathbf{x} = (x, y, z) \in \bar{\Omega} : x = 1\}, \quad \Gamma_D = \partial\Omega \setminus \Gamma_N.$$

The diffusion tensor is

$$\mathcal{K}(\boldsymbol{\mu}) = \mathcal{K}(\mathbf{x}; \boldsymbol{\mu}) = \nu(\mathbf{x}; \boldsymbol{\mu}) \text{diag}(1, 1, 10^{-2}),$$

where $\nu(\mathbf{x}; \boldsymbol{\mu})$ is the piecewise constant on four subregions $\Omega_1 = (0, 1) \times (0, 0.5) \times (0, 0.5)$, $\Omega_2 = (0, 1) \times (0, 0.5) \times (0.5, 1)$, $\Omega_3 = (0, 1) \times (0.5, 1) \times (0, 0.5)$, and $\Omega_4 = (0, 1) \times (0.5, 1) \times (0.5, 1)$, denoted by

$$\nu(\mathbf{x}; \boldsymbol{\mu}) = \begin{cases} \mu_j, & \mathbf{x} \in \Omega_j, \quad j = 1, \dots, 3, \\ 1, & \mathbf{x} \in \Omega_4. \end{cases}$$

We consider the following parameter-dependent Gaussian function as the source term

$$f(\mathbf{x}; \boldsymbol{\mu}) = \mu_7 + \frac{\exp(-((x - \mu_4)^2 + (y - \mu_5)^2 + (z - \mu_6)^2)/\mu_7)}{\mu_7},$$

and homogeneous boundary conditions

$$g_D(\boldsymbol{\mu}) = 0, \quad g_N(\boldsymbol{\mu}) = 0.$$

The 7-dimensional parameter domain is $\mathcal{D} = [0.1, 1]^3 \times [0.4, 0.6]^3 \times [0.25, 0.5]$.

4.1 Results on convergence and efficiency of RBWS

For both examples, linear finite elements as implemented in the Matlab package iFEM [6] with DoFs $\mathcal{N} = 35,937$ are adopted as the high-fidelity discretization. Subsequently, we employ the three methods detailed in Table 1 to solve the resulting discrete system (1). For the MGCG method and the RBI-MGCG method, we use an MG method with

Method	Iterative solver	Initial guess
MGCG	MGCG (Section 2.2)	$u_h^{(0)}(\boldsymbol{\mu}) = 0$
RBI-MGCG	MGCG (Section 2.2)	$u_h^{(0)}(\boldsymbol{\mu}) = \text{RBM}_{\text{L1ROC}}(A_h(\boldsymbol{\mu}), f_h(\boldsymbol{\mu}), N)$
RBI-MSRBCG	MSRBCG (Section 2.3)	$u_h^{(0)}(\boldsymbol{\mu}) = \text{RBM}_{\text{POD}}(A_h(\boldsymbol{\mu}), f_h(\boldsymbol{\mu}), N)$

Table 1: Three methods tested in this paper.

4 levels ($J = 3$) as the preconditioner. The L1ROC method is used for the initialization of the RBI-MGCG method. The POD-based RBM is used for the initialization of the RBI-MSRBCG method. Here we consider a fixed RB dimension N for the MSRBCG preconditioners at each iteration step, i.e., $N^{(k)} = N$.

For Example 1, 70 parameters are sampled by the popular Latin hypercube sampling (LHS) method [22] to build the training set Ξ_{train} for the L1ROC method and

POD-based RBM. Then we respectively construct the RB spaces of different dimensions $N = 10, 15, 20$ and test the corresponding RBM initialized iterative methods. The parametrized linear system is solved for a testing set Ξ_{test} consisting of 500 parameters with the residual tolerance $\delta = 10^{-16}$ and the maximum number of iterations $L_{\text{max}} = 40$. To eliminate the parametric variations, we calculate the average value of the norms of all relative residuals

$$r_{\text{ave}}^{(k)} = \frac{\sum_{\boldsymbol{\mu} \in \Xi_{\text{test}}} \|r_h^{(k)}(\boldsymbol{\mu})\| / \|f_h(\boldsymbol{\mu})\|}{\#\Xi_{\text{test}}},$$

where $r_h^{(k)}(\boldsymbol{\mu}) = f_h(\boldsymbol{\mu}) - A_h(\boldsymbol{\mu})u_h^{(k)}(\boldsymbol{\mu})$. And the convergence results of the average residual $r_{\text{ave}}^{(k)}$ as a function of the iteration k are presented in Figure 1 top left. We can see that the RBM-initialized methods starting from more accurate initial values require fewer iterations than the method without such a warm start. The MSRB preconditioner could provide a significant acceleration for the CG method within a certain precision. However, when the accuracy increases further, the MSRB preconditioner is significantly degraded, which leads to a much slower convergence. This is consistent with what our formal analysis in Section 3.2.1 predicts.

To demonstrate the efficiency benefit brought by the RBWS method, we record the cumulative runtime as the number of linear solves increases, which is shown in Figure 1 top right. The values corresponding to zero solves represent the computational cost of the offline training process. It can be seen that the RBI-MGCG methods begin to pay off quickly when the parametrized system is solved about 60 times thanks to its high online-efficiency. For the RBI-MSRB methods, the construction of the MSRB preconditioners is much more time-consuming and generates much less marginal savings online compared with the RBI-MGCG method. For a more detailed comparison, we report in Tabel 2 the break-even point (BEP) for the two RBWS methods that is defined as

$$\text{BEP} = \frac{t_{\text{off}}}{t_{\text{on}}(\text{MGCG}) - t_{\text{on}}(\text{RBWS})}.$$

Here, t_{off} denotes the computation time for the offline stage, while t_{on} means the average computation time for the online stage. We specify two different values for the tolerance δ and record the iteration step number L required for the average residual $r_{\text{ave}}^{(k)}$ to fall below δ . We see that the advantage of RBM preconditioning (adopted by RBI-MSRBCG) disappears when we move from low ($\delta = 10^{-8}$) to high ($\delta = 10^{-16}$) precision.

For Example 2, we build the RB spaces of dimensions $N = 100, 200, 300$ based on 500 training parameters for the L1ROC method and POD-based RBM respectively, and test all methods for 30,000 testing parameters. The results of the convergence and the cumulative time are presented in the bottom row of Figure 1. And the the comparison results of L , t_{off} , t_{on} , and BEP are shown in Table 3. The comparison of RBI-MGCG and RBI-MSRBCG is consistent with Example 1.

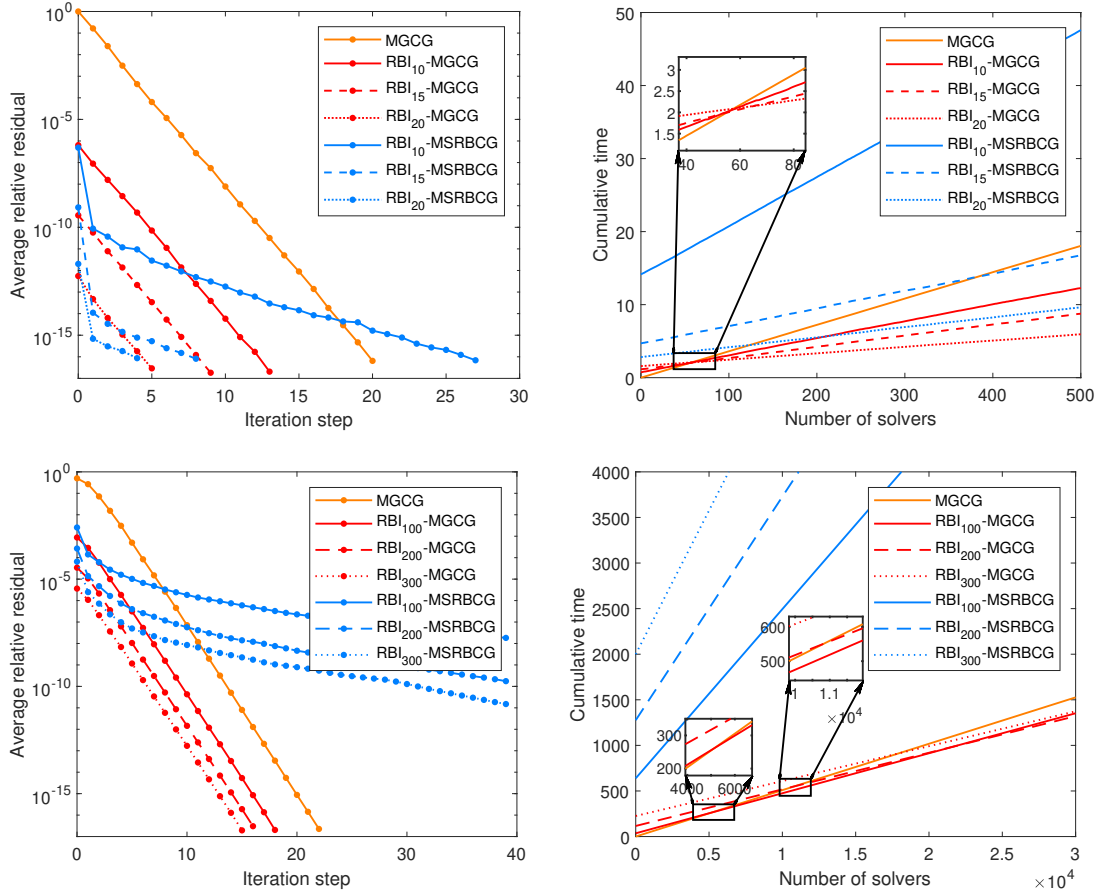


Figure 1: Left: The convergence result with the iteration. Right: The total computational cost as the number of online solvers increases. (Top: Example 1, Bottom: Example 2.)

Method	N	$\delta = 10^{-8}$				$\delta = 10^{-16}$			
		L	t_{off}	t_{on}	BEP	L	t_{off}	t_{on}	BEP
MGCG	–	10	–	1.87E-02	–	20	–	3.61E-02	–
RBI-MGCG	10	3	7.31E-01	7.10E-03	61	13	7.31E-01	2.30E-02	58
	15	0	1.15E00	8.26E-04	63	9	1.15E00	1.52E-02	56
	20	0	1.58E00	9.32E-04	86	5	1.58E00	8.79E-03	59
RBI-MSRBCG	10	1	6.86E-01	4.62E-03	49	27	1.41E01	6.63E-02	∞
	15	0	8.92E-02	1.54E-03	7	8	4.70E00	2.39E-02	383
	20	0	9.51E-02	1.72E-03	7	4	2.82E00	1.38E-02	125

Table 2: Detailed results with different $\delta = 10^{-8}, 10^{-16}$ for Example 1

Method	N	$\delta = 10^{-8}$				$\delta = 10^{-16}$			
		L	t_{off}	t_{on}	BEP	L	t_{off}	t_{on}	BEP
MGCG	–	11	–	1.49E-02	–	22	–	2.67E-02	–
RBI-MGCG	100	7	3.56E01	1.04E-02	3929	18	3.56E01	2.20E-02	5132
	200	6	1.16E02	8.63E-03	9248	16	1.16E02	2.01E-02	10829
	300	4	2.26E02	7.58E-03	15374	15	2.26E02	1.91E-02	17910
RBI-MSRBCG	100	≥ 40	$\geq 6.39\text{E}02$	$\geq 9.45\text{E-}02$	–	≥ 40	$\geq 6.39\text{E}02$	$\geq 9.28\text{E-}02$	–
	200	17	5.45E02	6.57E-02	∞	≥ 40	$\geq 1.28\text{E}03$	$\geq 1.23\text{E-}02$	–
	300	10	4.66E02	5.19E-02	∞	≥ 40	$\geq 2.00\text{E}03$	$\geq 1.58\text{E-}02$	–

Table 3: Detailed results with different $\delta = 10^{-8}, 10^{-16}$ for Example 2

4.2 Numerical confirmation of the efficiency degradation of the RB preconditioner

To confirm our analysis in Section 3.2.1, we estimate the approximation accuracy of the RB space by computing the maximum relative residual of the RB solutions solved by (8) over the test set,

$$r_N = \max_{\boldsymbol{\mu} \in \Xi_{\text{test}}} \frac{\|f_h(\boldsymbol{\mu}) - A_h(\boldsymbol{\mu})u_h^{rb}(\boldsymbol{\mu})\|}{\|f_h(\boldsymbol{\mu})\|}.$$

The convergence of r_N with the RB dimension N is presented in Figure 2. Comparing the approximation accuracy of the RB space with the convergence results of the RBI-MSRBCG methods in Figure 1, we can conclude that the preconditioner starts to be less efficient shortly after the iterative accuracy exceeds the approximation accuracy of the RB space. Moreover, we check the decay rate of the Kolmogorov n -width of the residual manifold $d_h^k = d_n(\mathcal{R}^{(k)})$ by running a POD on the residual snapshot collection

$$\overline{\mathcal{R}}^{(k)} := \left\{ r_h^{(k-\frac{1}{2})}(\boldsymbol{\mu}) = f_h(\boldsymbol{\mu}) - A_h(\boldsymbol{\mu})u_h^{(k-\frac{1}{2})}(\boldsymbol{\mu}) : \boldsymbol{\mu} \in \Xi_{\text{train}} = \{\boldsymbol{\mu}_n\}_{n=1}^{n_s} \right\},$$

which are obtained by the RBI-MSRBCG method with the RB dimension $N = 20$ for Example 1 and $N = 300$ for Example 2. The rate of decay of the relative eigenvalues λ_n/λ_{\max} is demonstrated in Figure 3. It's clear that the relative eigenvalues decay fast during the first two iterations, and decrease much slower as the iteration goes on.

5 Conclusion

We propose and test a reduced basis warm-start approach employing a highly efficient RBM variant to initialize the high-fidelity iterative method to obtain the high-precision solutions of the parametrized linear systems. Moreover, we discuss the efficiency limitation of RBM, for situations when solutions with machine accuracy are sought, and when it is adopted as a preconditioner in the iterative methods. The numerical results demonstrate the advantage of the RBWS initialization and verify the limitation of RBM as a preconditioner.

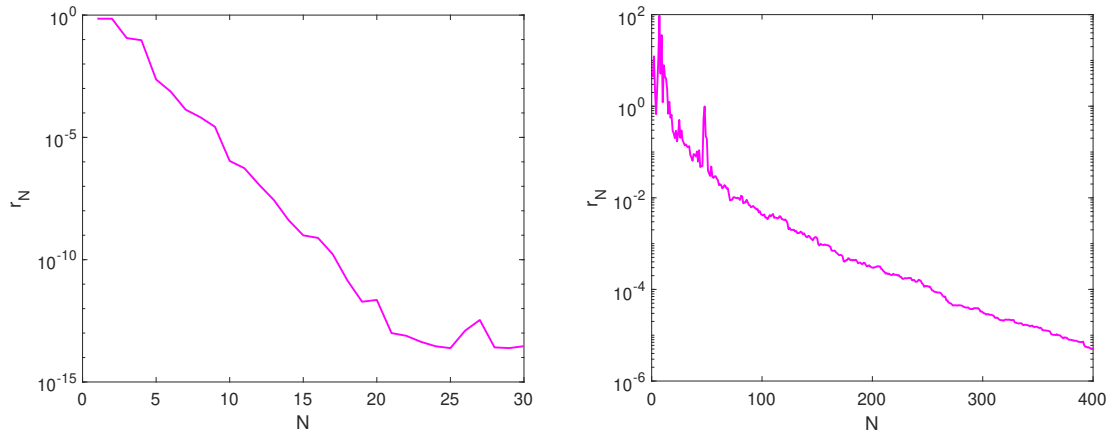


Figure 2: The convergence of the relative residual r_N with the RB dimension N . (Left: Example 1, Right: Example 2.)

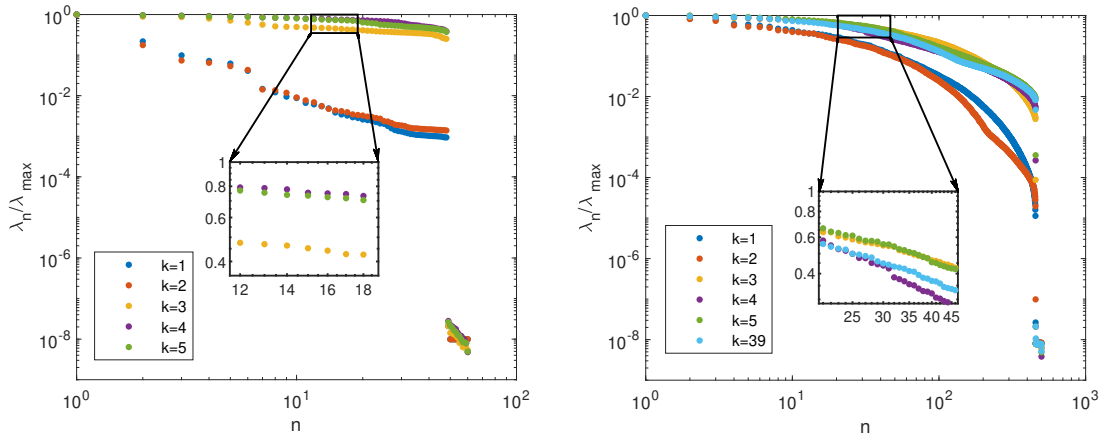


Figure 3: Decay of the eigenvalues for the residual snapshots computed by the RBI-MSRBCG method. (Left: Example 1, Right: Example 2.)

References

- [1] M. Barrault, Y. Maday, N. C. Nguyen, and A. T. Patera. An ‘empirical interpolation’ method: application to efficient reduced-basis discretization of partial differential equations. *C. R. Math. Acad. Sci. Paris*, 339(9):667–672, 2004.
- [2] P. Binev, A. Cohen, W. Dahmen, R. DeVore, G. Petrova, and P. Wojtaszczyk. Convergence rates for greedy algorithms in reduced basis methods. *SIAM J. Math. Anal.*, 43(3):1457–1472, 2011.
- [3] A. Brandt. Multi-level adaptive solutions to boundary-value problems. *Math. Comp.*, 31(138):333–390, 1977.
- [4] A. Buffa, Y. Maday, A. T. Patera, C. Prud’homme, and G. Turinici. *A priori* convergence of the greedy algorithm for the parametrized reduced basis method. *ESAIM Math. Model. Numer. Anal.*, 46(3):595–603, 2012.
- [5] S. Chaturantabut and D. C. Sorensen. Nonlinear model reduction via discrete empirical interpolation. *SIAM J. Sci. Comput.*, 32(5):2737–2764, 2010.
- [6] L. Chen. An integrated finite element method package in matlab. *California: University of California at Irvine*, 2009.
- [7] Y. Chen, S. Gottlieb, L. Ji, and Y. Maday. An EIM-degradation free reduced basis method via over collocation and residual hyper reduction-based error estimation. *J. Comput. Phys.*, 444:Paper No. 110545, 18, 2021.
- [8] Y. Chen, L. Ji, A. Narayan, and Z. Xu. L1-based reduced over collocation and hyper reduction for steady state and time-dependent nonlinear equations. *J. Sci. Comput.*, 87(1):Paper No. 10, 21, 2021.
- [9] Y. Chen, J. Jiang, and A. Narayan. A robust error estimator and a residual-free error indicator for reduced basis methods. *Comput. Math. Appl.*, 77(7):1963–1979, 2019.
- [10] A. Cohen, W. Dahmen, R. DeVore, and J. Nichols. Reduced basis greedy selection using random training sets. *ESAIM Math. Model. Numer. Anal.*, 54(5):1509–1524, 2020.
- [11] N. Dal Santo, S. Deparis, A. Manzoni, and A. Quarteroni. Multi space reduced basis preconditioners for large-scale parametrized PDEs. *SIAM J. Sci. Comput.*, 40(2):A954–A983, 2018.
- [12] N. Dal Santo, S. Deparis, A. Manzoni, and A. Quarteroni. Multi space reduced basis preconditioners for parametrized Stokes equations. *Comput. Math. Appl.*, 77(6):1583–1604, 2019.

- [13] R. DeVore, G. Petrova, and P. Wojtaszczyk. Greedy algorithms for reduced bases in Banach spaces. *Constr. Approx.*, 37(3):455–466, 2013.
- [14] B. Haasdonk. Reduced basis methods for parametrized PDEs—a tutorial introduction for stationary and instationary problems. In *Model reduction and approximation*, volume 15 of *Comput. Sci. Eng.*, pages 65–136. SIAM, Philadelphia, PA, 2017.
- [15] W. Hackbusch. *Multi-grid methods and applications*, volume 4. Springer Science & Business Media, 2013.
- [16] M. R. Hestenes and E. Stiefel. Methods of conjugate gradients for solving linear systems. *J. Research Nat. Bur. Standards*, 49:409–436, 1952.
- [17] J. S. Hesthaven, G. Rozza, and B. Stamm. *Certified reduced basis methods for parametrized partial differential equations*. SpringerBriefs in Mathematics. Springer, Cham; BCAM Basque Center for Applied Mathematics, Bilbao, 2016. BCAM SpringerBriefs.
- [18] P. Holmes, J. L. Lumley, and G. Berkooz. *Turbulence, coherent structures, dynamical systems and symmetry*. Cambridge Monographs on Mechanics. Cambridge University Press, Cambridge, 1996.
- [19] T. Kadeethum, D. O’malley, F. Ballarin, I. Ang, J. N. Fuhg, N. Bouklas, V. L. Silva, P. Salinas, C. E. Heaney, C. C. Pain, et al. Enhancing high-fidelity nonlinear solver with reduced order model. *Sci. Rep.*, 12(1):20229, 2022.
- [20] C. T. Kelley. *Iterative methods for linear and nonlinear equations*, volume 16 of *Frontiers in Applied Mathematics*. Society for Industrial and Applied Mathematics (SIAM), Philadelphia, PA, 1995. With separately available software.
- [21] Y. Liang, H. Lee, S. Lim, W. Lin, K. Lee, and C. Wu. Proper orthogonal decomposition and its applications—Part I: Theory. *J. Sound Vib.*, 252(3):527–544, 2002.
- [22] M. D. McKay, R. J. Beckman, and W. J. Conover. A comparison of three methods for selecting values of input variables in the analysis of output from a computer code. *Technometrics*, 21(2):239–245, 1979.
- [23] N.-C. Nguyen and Y. Chen. Reduced-basis method for the iterative solution of parametrized symmetric positive-definite linear systems. *arXiv preprint arXiv:1804.06363*, 2018.
- [24] S. Nikolopoulou, I. Kalogerisa, G. Stavroulakisa, and V. Papadopoulou. Ai-enhanced iterative solvers for accelerating the solution of large-scale parametrized systems. *arXiv preprint arXiv:2207.02543*, 2022.

- [25] A. Quarteroni, A. Manzoni, and F. Negri. *Reduced basis methods for partial differential equations: An introduction*, volume 92. Springer, 01 2015.
- [26] G. Rozza, D. B. P. Huynh, and A. T. Patera. Reduced basis approximation and a posteriori error estimation for affinely parametrized elliptic coercive partial differential equations: application to transport and continuum mechanics. *Arch. Comput. Methods Eng.*, 15(3):229–275, 2008.
- [27] Y. Saad and M. H. Schultz. GMRES: a generalized minimal residual algorithm for solving nonsymmetric linear systems. *SIAM J. Sci. Statist. Comput.*, 7(3):856–869, 1986.
- [28] O. Tatebe. The multigrid preconditioned conjugate gradient method. In *NASA Langley Research Center, The Sixth Copper Mountain Conference on Multigrid Methods, Part 2*, 1993.
- [29] H. A. van der Vorst. Bi-CGSTAB: a fast and smoothly converging variant of Bi-CG for the solution of nonsymmetric linear systems. *SIAM J. Sci. Statist. Comput.*, 13(2):631–644, 1992.
- [30] M. Zhou, J. Han, M. Rachh, and C. Borges. A neural network warm-start approach for the inverse acoustic obstacle scattering problem. *J. Comput. Phys.*, 490:Paper No. 112341, 16, 2023.

A The estimate of the computational cost of the offline stage

In this section, we give an estimation of the computational cost of the greedy-based RBM and illustrate the cost challenge of developing high-precision RB solutions. Let $\mathcal{M} = \{u(\boldsymbol{\mu}) : \boldsymbol{\mu} \in \mathcal{D}\}$ denote the solution manifold consisting of all parameter-dependent solutions. Here we first recall an essential definition in the numerical analysis of the RBM, the Kolmogorov n -width, indicating the difference between the optimal n -dimensional linear approximation space and the solution manifold \mathcal{M}

$$d_n = d_n(\mathcal{M}) = \inf_{\dim(\mathcal{L})=n} \sup_{u(\boldsymbol{\mu}) \in \mathcal{M}} \text{dist}(u(\boldsymbol{\mu}), \mathcal{L}),$$

where \mathcal{L} denotes the n -dimensional linear approximation spaces. Assuming the RB space W_n of dimension n is built by the weak greedy algorithm, we denote the following approximation error

$$\sigma_n = \sigma_n(\mathcal{M}) = \max_{u(\boldsymbol{\mu}) \in \mathcal{M}} \|u(\boldsymbol{\mu}) - P_{W_n} u(\boldsymbol{\mu})\|_V,$$

where P_{W_n} is the projection operator on W_n . It was proved in [2, 13, 4] that any polynomial rate of decay achieved by the Kolmogorov n -width d_n is retained by the approximation error σ_n . Precisely, the following holds, see [2, Theorem 3.1].

Theorem 1. For $M > 0$ and $s > 0$, suppose that $d_n(\mathcal{M}) \leq M(\max\{1, n\})^{-s}$, $n \geq 0$. We have $\sigma_n(\mathcal{M}) \leq M_s \gamma^{-2} (\max\{1, n\})^{-s}$, where $M_s = 2^{4s+1}M$, and γ is a positive threshold parameter independent of n in the weak greedy algorithm.

To achieve a target accuracy ε , with Theorem 1, an estimate on the number of greedy steps $n(\varepsilon)$ was provided in [10, Corollary 2.4], as follows

Corollary 1. For $M > 0$ and $s > 0$, suppose that $d_n(\mathcal{M}) \leq M(\max\{1, n\})^{-s}$, $n \geq 0$. We have $n(\varepsilon) \leq M_1 \varepsilon^{-1/s}$, $\varepsilon > 0$, where M_1 depends on M , s and greedy parameter γ .

In the practical calculation, the greedy algorithm is applied based on a discrete training parameter set $\tilde{\mathcal{D}}$ instead of the continuous parameter set \mathcal{D} . In [10], the authors also estimated the size of $\tilde{\mathcal{D}}$ under the assumption

$$\|u_h(\boldsymbol{\mu}_1) - u_h(\boldsymbol{\mu}_2)\| \leq M \|\boldsymbol{\mu}_1 - \boldsymbol{\mu}_2\|, \quad \boldsymbol{\mu}_1, \boldsymbol{\mu}_2 \in \mathcal{D}, \quad M > 0.$$

They showed that the discrete manifold $\tilde{\mathcal{M}} = \{u(\boldsymbol{\mu}) : \boldsymbol{\mu} \in \tilde{\mathcal{D}}\}$ should be a ε -net² of the manifold \mathcal{M} for the target accuracy ε . Such $\tilde{\mathcal{M}}$ could be induced by a $M^{-1}\varepsilon$ -net of \mathcal{D} that scales like $\#\tilde{\mathcal{D}} \sim \varepsilon^{-cp}$. The size $\#\tilde{\mathcal{D}}$ in conjunction with the number of greedy steps $n(\varepsilon)$ shows that the total number of error estimator evaluations is at best of the order $\mathcal{O}(\varepsilon^{-cp/s})$.

The offline cost mainly includes two parts, the cost of computing $n(\varepsilon)$ FOM solutions each of dimension \mathcal{N} and the cost of computing the error estimators based on the RB space of dimension $N = n(\varepsilon)$. Thus the total offline cost scales like

$$\text{Poly}(\mathcal{N})n(\varepsilon) + \text{Poly}(N)\mathcal{O}(\varepsilon^{-cp/s}).$$

Given an exponential accuracy $\varepsilon = 10^{-a}$, we can find that the offline cost increases exponentially as the accuracy parameter a and the parameter dimension p increase and the parameter s that indicates the decay rate of the Kolmogorov width decreases.

²If $\tilde{\mathcal{M}}$ satisfies $\mathcal{M} \subset \bigcup_{u(\boldsymbol{\mu}) \in \tilde{\mathcal{M}}} B(u(\boldsymbol{\mu}), \delta)$, $\tilde{\mathcal{M}}$ is called a δ -net of \mathcal{M} .